

PAPER

## Facile fabrication of ZnO—graphite composite thin films for ultraviolet photodetection

To cite this article: Medini Padmanabhan *et al* 2018 *Mater. Res. Express* **5** 095606

View the [article online](#) for updates and enhancements.

### Related content

- [Sandwiched assembly of ZnO nanowires between graphene layers for a self-powered and fast responsive ultraviolet photodetector](#)

Buddha Deka Boruah, Anwesha Mukherjee and Abha Misra

- [Fabrication of -Ga<sub>2</sub>O<sub>3</sub>/ZnO heterojunction for solar-blind deep ultraviolet photodetection](#)

D Y Guo, H Z Shi, Y P Qian *et al.*

- [Few-layer graphene/ZnO nanowires based high performance UV photodetector](#)

Buddha Deka Boruah, Darim B Ferry, Anwesha Mukherjee *et al.*



**IOP | ebooks™**

Bringing you innovative digital publishing with leading voices to create your essential collection of books in STEM research.

Start exploring the collection - download the first chapter of every title for free.

# Materials Research Express



## PAPER

RECEIVED  
16 June 2018

REVISED  
19 July 2018

ACCEPTED FOR PUBLICATION  
2 August 2018

PUBLISHED  
17 August 2018

## Facile fabrication of ZnO–graphite composite thin films for ultraviolet photodetection

Medini Padmanabhan , Rachel Meyen and Kerri Houghton

Physical Sciences Department, Rhode Island College, Providence RI-02908, United States of America

E-mail: [mpadmanabhan@ric.edu](mailto:mpadmanabhan@ric.edu)

**Keywords:** thin films, composite, photodetector, carbon

Supplementary material for this article is available [online](#)

### Abstract

We present a facile method for the fabrication of ZnO-graphite composite thin films by using the technique of interface exfoliation. Natural graphite and ZnO are trapped at an oil–water interface, resulting in the exfoliation of graphite and formation of a composite. These thin films exhibit photoconductivity in the presence of ultraviolet radiation. The extent of the response and the time scales involved depend on the relative amount of ZnO and graphite, which is determined by fabrication conditions. We focus on using commercially available, non-toxic materials for the entire fabrication route.

### 1. Introduction

Ever since its discovery, graphene has commanded considerable interest in the field of optoelectronics. Pristine graphene has proven itself to be a fast and versatile photodetector suitable for some niche applications [1]. However, the quest has been ongoing in identifying and developing alternate device structures amenable to cost-effective, large-scale production. Combining graphene with functional elements has resulted in a new variety of heterostructures and composites which integrate desirable properties of both the constituents. Methods for graphene functionalization range from covalent attachment to simple contact. Devices such as photodetectors, solar cells and photocatalytic hydrogen generators have been developed based on this concept [2].

ZnO is a material whose band structure makes it uniquely suited for ultraviolet (UV) photodetection [3]. Indeed, many device architectures have been attempted in order to achieve high detection levels and fast response times. Nano structuring has proven to be a valuable tool in achieving desirable device performance. Recently, attempts have been made to functionalize graphene with ZnO with the hopes of combining the photoabsorptive characteristics of ZnO and high electron mobility of graphene. The presence of a high mobility component is expected to increase photocurrents and decrease response times. Device architectures that have been attempted include vertically aligned nanowires [4, 5], heterostructures [6, 7], and composites [8–10]. The variation in the crystalline qualities of ZnO and graphene, as well as the multitude of architectures resulting in different types of interfaces have given rise to a wide range of device performance metrics. While ZnO nanowires have been studied due to the availability of a long crystalline pathway [11], carbon nanodots have proven to be quite effective in enhancing device performance [12, 13]. Of all the device architectures, composites are of particular interest due to the close proximity of the constituent materials.

In this work, we present facile, one-step integration of ZnO particles into graphitic thin films by using solvent interface trapping and exfoliation. This technique, pioneered in [14], is a promising method which has yielded large area, transparent, conducting graphene films. The method exploits the fact that the surface energy of graphene lies in between the values of surface tensions for water and heptane. This results in the trapping and exfoliation of natural graphite to graphene films one to four layers thick [14]. The combination of minimal physical agitation and lack of chemical modification is expected to retain the desirable properties of pristine graphene. Here, we extend this technique by introducing ZnO nanoparticles into the water phase, thereby incorporating them into the thin films. We find that ZnO-graphite composite films are formed with relative

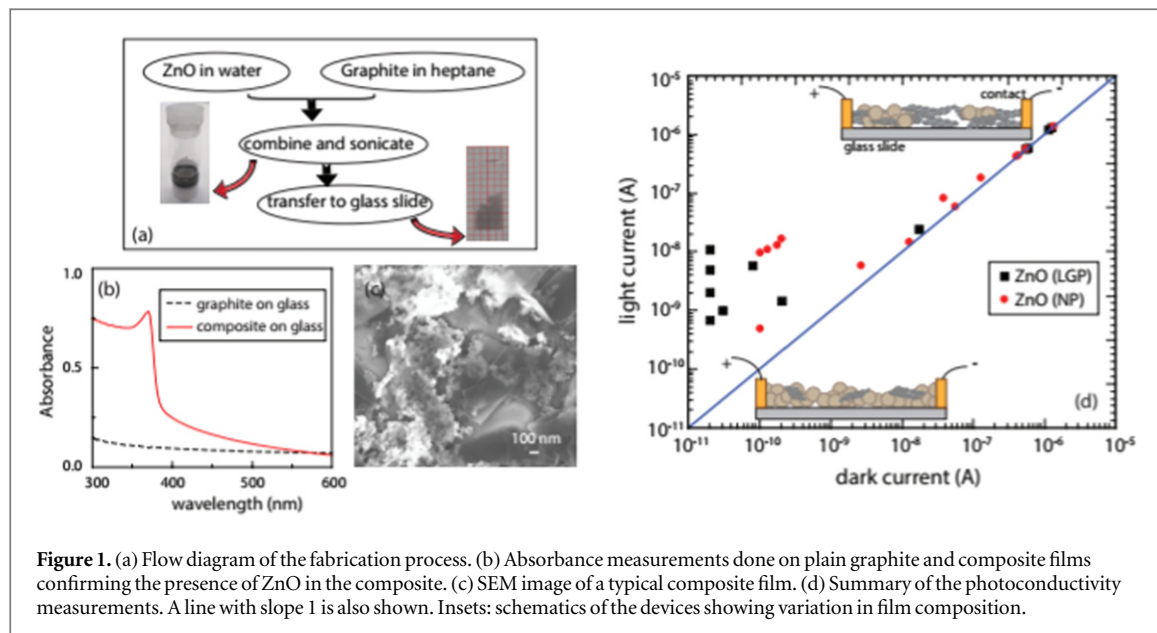


**Figure 1.** (a) Flow diagram of the fabrication process. (b) Absorbance measurements done on plain graphite and composite films confirming the presence of ZnO in the composite. (c) SEM image of a typical composite film. (d) Summary of the photoconductivity measurements. A line with slope 1 is also shown. Insets: schematics of the devices showing variation in film composition.

ease. By varying the amount of constituents in the liquid phases, we can tune the composition of these films from ZnO-rich to graphite-rich. The UV photodetection characteristics of these devices are found to be strongly dependent on this relative ratio.

We would like to emphasize that the materials used in this study are all commercially available. Our goal is to combine these components by using facile, non-toxic fabrication methods and develop functional composite materials.

## 2. Methods

A schematic of our fabrication process is shown in figure 1(a). The starting material for our fabrication is natural graphite flakes (Asbury Carbons-3243). A small quantity ( $\sim 1\text{--}3$  mg) is added to about 1.2 ml of heptane (Sigma Aldrich-246654) and sonicated in a bath sonicator to break up agglomerates. The mixture is allowed to sit for 30–120 s and 1 ml of the suspension is then transferred to a separate glass vial. 1 ml of water is then added to the vial. A small amount of ZnO is also added to the water. The contents are then sonicated in a bath or horn sonicator for about 30 s. At the end of this step, a thin film is seen to climb up the inner surface of the glass vial. A pre-cleaned glass slide is then inserted into the vial which results in it being coated with the film. Sometimes, a cotton applicator soaked in isopropanol is used to manually compact the films. The procedure is the same as the one outlined in [15]. An absorbance measurement using a UV–vis spectrometer shows enhanced absorption below 385 nm in the composite film due to the presence of ZnO (figure 1(b)).

Electrical contacts are made using conducting silver paste (Sigma Aldrich 735825). Typical area between two electrodes is  $3 \times 1 \text{ mm}^2$ . Two-point electrical measurements are done using a Keithley SMU 2400. A commercial UV-LED with a wavelength of 365 nm is used as the illumination source.

We would like to point out that two sources of ZnO are reported in this study: nanoparticles (NP, Sigma Aldrich 721077, average particle size  $\leq 40$  nm, 98% monoclinic) and laboratory grade powder (LGP, Horsehead Corporation). While the main motivation for trying out the LGP was reduction in starting material cost, the comparison has unveiled a dependence of film properties on the microstructure of ZnO.

## 3. Results and discussion

Figure 1(c) shows the SEM image of a typical sample. The proximity between ZnO particles and graphite flakes can clearly be seen. Although ample evidence is present for high levels of exfoliation, we have not been able to accurately measure the number of layers in our graphite flakes. In the absence of Raman and AFM data, we refer to our films as graphite (and not graphene) films in the rest of this manuscript.

Figure 1(d) summarizes the results of photoconductivity measurements performed on multiple samples. A constant bias of 1 V is applied across each sample and the current through the sample is measured in the absence ( $I_d$ ) and presence ( $I_l$ ) of UV light. As can be seen from the plot, depending on the fabrication details, the conductivities of our samples span many orders of magnitude. We observe that samples which have high values

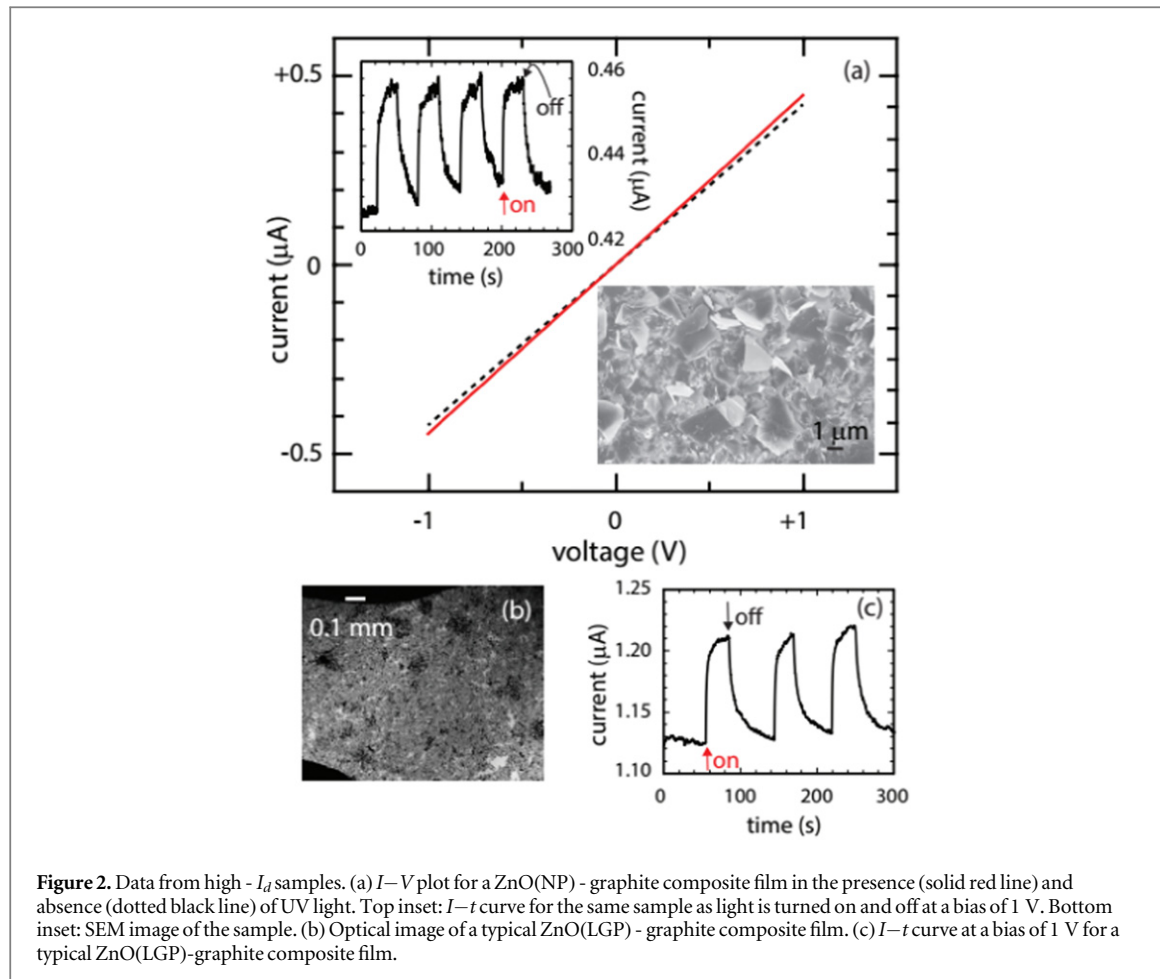


**Figure 2.** Data from high -  $I_d$  samples. (a)  $I$ – $V$  plot for a ZnO(NP) - graphite composite film in the presence (solid red line) and absence (dotted black line) of UV light. Top inset:  $I$ – $t$  curve for the same sample as light is turned on and off at a bias of 1 V. Bottom inset: SEM image of the sample. (b) Optical image of a typical ZnO(LGP) - graphite composite film. (c)  $I$ – $t$  curve at a bias of 1 V for a typical ZnO(LGP)-graphite composite film.

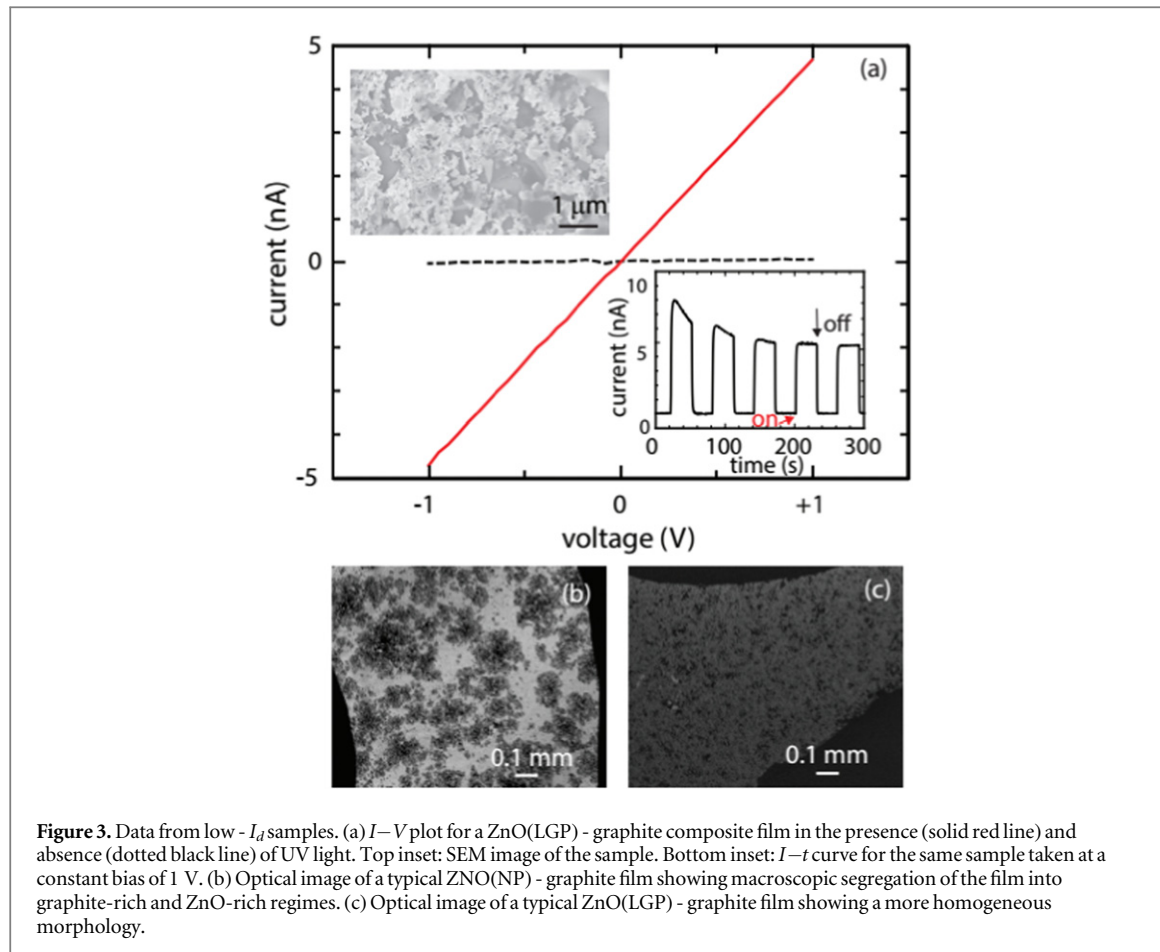
of  $I_d$  undergo a few percent change in the current as a result of illumination. However, in the case of films with low values of  $I_d$ , illumination causes an increase in the current up to two orders of magnitude. The line shown corresponds to the condition:  $I_l = I_d$ . Schematics representing variation of film composition as we move from the ‘low- $I_d$ ’ to the ‘high- $I_d$ ’ regimes are shown as insets to figure 1(d). In the rest of the manuscript, we present detailed results and discussion from both the high -  $I_d$  and low -  $I_d$  domains.

In figure 2(a), we present data from a ZnO(NP)-graphite composite film with a dark current of about  $0.43 \mu\text{A}$  at a bias of 1 V. The high value of  $I_d$  is consistent with the SEM image (inset of figure 2(a)) where graphite flakes are shown to be in contact with each other. It would be safe to assume that the dominant conducting channel is this interconnected network of graphite flakes. The close contact between ZnO and these flakes allow a facile transfer of charge when photogenerated carriers are induced in ZnO as a result of UV illumination. The current-voltage ( $I$ – $V$ ) data for this sample in the presence and absence of light is shown in figure 2(a). We observe that the response is linear in both cases with a 5% increase in conductivity as a result of illumination. The timescales involved in the photoresponse can be studied by monitoring the current through the sample at a constant bias while turning the light source on and off ( $I$ – $t$  curve). This data is presented in the top inset which shows a rise time of 2 s and fall time of 17 s.

In figure 2(c) we show similar data from a ZnO(LGP)-graphite composite sample. Again, the value of  $I_d$  is high, suggesting transport through graphite layer. A current change of 7% is observed in response to UV light. The optical image of a LGP-graphite sample is shown in figure 2(b). Major defects include tears and clustering of thick graphite flakes. Within the resolution of our experiments, no significant differences are observed in the optical images or electrical data of NP and LGP films. We conclude that the microstructure of the additive does not affect the properties of these high  $I_d$  samples.

While it is tempting to conclude that what we observe in figure 2 is a result of charge transfer from ZnO to graphite, we have to consider the possibility that we are just observing the effects of having two resistors in parallel. However, considering the thorough intermixing of graphite and ZnO as observed in our SEM images, we conclude that it is unlikely that they form independent conducting channels.

In figure 3, we present data from samples which exhibit low values of  $I_d$  (of the order of  $10^{-11}$  to  $10^{-10} \text{ A}$ ). The nature of the additive (NP versus LGP) seems to have a substantial effect on the properties of the low  $I_d$  samples. Low- $I_d$  films fabricated with ZnO(NP) do not show uniform morphology. As shown in the optical



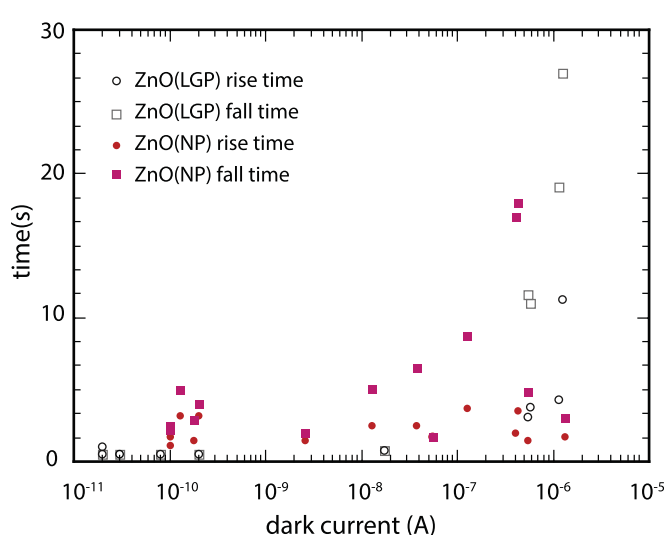
**Figure 3.** Data from low -  $I_d$  samples. (a)  $I-V$  plot for a ZnO(LGP) - graphite composite film in the presence (solid red line) and absence (dotted black line) of UV light. Top inset: SEM image of the sample. Bottom inset:  $I-t$  curve for the same sample taken at a constant bias of 1 V. (b) Optical image of a typical ZnO(NP) - graphite film showing macroscopic segregation of the film into graphite-rich and ZnO-rich regimes. (c) Optical image of a typical ZnO(LGP) - graphite film showing a more homogeneous morphology.

image in figure 3(b), the films segregate into graphite-rich and ZnO-rich phases on a macroscopic scale. On the other hand, LGP-graphite films are easy to fabricate and maintain their uniformity over large areas (optical image shown in figure 3(c)).

Figure 3(a) shows data from a ZnO(LGP)-graphite sample. The SEM image (top inset) shows a film which is predominantly ZnO with graphite flakes interspersed in the ZnO matrix. Most of current conduction is presumably happening via the ZnO network. Illumination with UV light results in an appreciable photoconductivity which manifests as a 250-fold increase in the current. The corresponding current-voltage diagram is shown in figure 3(a). The dark curve is almost flat while the light curve shows linear behavior. The response of the sample as light is turned on and off is shown in the bottom inset. In contrast to figure 2, response times are much faster (0.5 s–1 s).

Response time is an important figure of merit for photodetectors. The functional form of the time dependence can give valuable information about the charge transfer processes happening in the system. In figure 4, we present data which summarizes the timescales observed in our measurements. Note that the response behavior of our photodetectors do not follow any specific functional form such as an exponential or bi-exponential. Hence, we define rise time as the time taken by the signal to reach 80% of its maximum value (above the base line) once the light is turned on. Similarly, we define fall time as the time taken by the signal to drop down to 20% of its maximum value once the light is turned off. We observe that fall times are almost always longer than rise times suggesting that the charge is quicker to build up than to dissipate. This is not surprising given that the charge traps in ZnO are known to affect the dynamics of photoresponse [16, 17]. We also see that NP films are generally slower in responding to light compared to LGP films-possibly due to their high surface-to-volume ratio accentuating the influence of surface trap states.

As seen in figure 4, samples with very low  $I_d$ , in which we expect the conduction to be dominated by the ZnO network, seem to have the lowest values of rise and fall times. To compare these with bare ZnO films, we dropcast ZnO onto glass slides and measured their photoresponse (data shown in supplementary information is available online at [stacks.iop.org/MRX/5/095606/mmedia](https://stacks.iop.org/MRX/5/095606/mmedia)). We observe that the timescales are roughly the same as the composite material. Although the addition of graphite does not affect the timescale of the response significantly, it is possible that the on/off ratio in the composite material is higher because of the presence of a more conducting phase. However, we are unable to make a quantitative comparison because the current values



**Figure 4.** Summary of the photoresponse timescales observed in our samples. Rise (fall) time is defined as the time taken by the photoresponse signal to reach 80 (20)% of its maximum value.

in the dropcast films depend critically on uniformity, thickness and porosity. It is not easy to make a dropcast film with the same parameters as the composite.

In figure 4, as the percentage of graphite increases (higher values of  $I_d$ ), we observe an increase in the response time scales. This is similar to data reported in [10], where a larger carbon: ZnO ratio results in longer response times. This is consistent with the theory that oxygen molecules need easy access to ZnO surface in order to influence charge build-up and dissipation [10]. We would however, like to point out that in [8], the authors achieve very fast response times ( $\sim 10$  ms) in a ZnO-graphene core–shell nanostructure device and attribute this to efficient charge transfer and high mobility.

Epitaxially grown pristine ZnO films are known to respond with very fast timescales [18, 19]. Any deviation from ideality, such as nanostructuring, seems to adversely affect the response speed, resulting in response times in the range of 10 s–100 s. The presence of atmospheric moieties such as oxygen and water vapor also have a marked influence on the photoresponse. It is widely accepted that oxygen molecules chemisorb on the surface of ZnO by accepting electrons. Illumination by UV light results in the formation of holes which reclaim these electrons, thereby leaving free electrons in the conduction band [16, 17].

While designing composites and heterostructures, one of the most important factors affecting charge transfer is the relative alignment of bands between the constituent materials [8, 20]. The work functions of pristine graphene and slightly n-type ZnO are so close together that any change in doping on either side can change the nature of the contacts from Ohmic to Schottky [21]. In our high  $I_d$  samples, we see Ohmic behavior in the presence and absence of light. In case of our low  $I_d$  samples, the behavior is again Ohmic in the presence of light. Please note that due to our device architecture, we are also probing the contact between ZnO and silver paste (low  $I_d$  samples) or graphite and silver paste (high  $I_d$  samples).

A common metric while discussing photodetectors is responsivity, defined as  $R = I_{photo}/PA$  where  $I_{photo}$  is the difference between the light and dark currents,  $P$  is the intensity of the illumination source and  $A$  is the area of the device [22]. The intensity of our UV LED at the distance at which we make measurements is  $5.7 \text{ mW cm}^{-2}$ . Plugging in values of  $A$ ,  $I_l$  and  $I_d$ , we obtain  $R = 1.3 \times 10^{-4} \text{ A W}^{-1}$  for the sample in figure 2(a) and  $R = 1.1 \times 10^{-5} \text{ A W}^{-1}$  for the sample in figure 3(a).

We would like to point out that these responsivities are lower than the best values reported in literature. In the case of bare ZnO, nanostructuring and temperature treatments have resulted in responsivities as high as  $71.7 \text{ AW}^{-1} \text{ V}^{-1}$  [23]. In case of ZnO-graphene core–shell nanocomposite structure, a responsivity of  $32 \text{ AW}^{-1} \text{ V}^{-1}$  was reported in [8]. There are multiple geometric and material factors which could lead to low values of responsivity in our samples. In literature, the preferred contact geometry is interdigitated electrodes. For a given resistivity, this design minimizes the ratio of length/area and allows for many resistors to be measured in parallel, thereby maximizing current output. Also, the usage of commercial ZnO in our study means that the crystallinity and particle size are not optimized for best performance. In addition, during the process of interface exfoliation, the individual graphite flakes resist sliding across each other. This results in a microscopically porous film where edges of individual flakes make contacts over small areas. This results in high junction resistance, thereby causing an overall decrease in the current flowing through the film. More work is required in order to figure out the optimum fabrication conditions.

## 4. Conclusions

In summary, we extend the technique of interface trapping and exfoliation to the fabrication of composite thin films. We find that ZnO particles are integrated into the graphite matrix with relative ease. The composition of the film can be varied by varying the amount of ZnO and graphite in this one-pot fabrication method. The resulting thin films show ultraviolet detection capabilities. The responsivities and timescales are shown to depend on the composition. While fabricating graphite-rich films, the microstructure of ZnO seems to have little effect on the homogeneity. However, in the case of ZnO-rich films, the LGP yields better quality films.

## Acknowledgments

MP is grateful to Prof Douglas Adamson, University of Connecticut for help with the technique of solvent interface trapping and exfoliation. Natural graphite used in this study was provided by Asbury Carbons, NJ. We thank Mr Charles Simpson, RIC for technical help and IMNI, Brown University for access to their SEM imaging facility, optical microscope and UV-vis spectrometer.

This work is supported in part by the National Science Foundation (grant number OIA-1538893). MP acknowledges support of Rhode Island College, Rhode Island College Foundation and Rhode Island College Alumni Affairs Ofifice.

## ORCID iDs

Medini Padmanabhan  <https://orcid.org/0000-0003-1593-3594>

## References

- [1] Sun Z and Chang H 2014 Graphene and graphene-like two-dimensional materials in photodetection: mechanisms and methodology *ACS Nano* **8** 4133–56
- [2] Gong X, Liu G, Li Y, Yu D Y W and Teoh W Y 2016 Functionalized-graphene composites: fabrication and applications in sustainable energy and environment *Chem. Mater.* **28** 8082–118
- [3] Peng L, Hu L and Fang X 2013 Low-dimensional nanostructure ultraviolet photodetectors *Adv. Mater.* **25** 5321–8
- [4] Zhang H, Babichev A V, Jacopin G, Lavenus P, Julien F H, Egorov A Y, Zhang J, Paupot T and Tchernycheva M 2013 Characterization and modeling of a ZnO nanowire ultraviolet photodetector with graphene transparent contact *J. Appl. Phys.* **114** 234505
- [5] Nie B *et al* 2013 Monolayer graphene film on ZnO nanorod array for high-performance Schottky junction ultraviolet photodetectors *Small* **9** 2872–9
- [6] Shao D, Gao J, Chow P, Sun H, Xin G, Sharma P, Lian J, Koratkar N A and Sawyer S 2015 Organic-inorganic heterointerfaces for ultrasensitive detection of ultraviolet light *Nano Lett.* **15** 3787–92
- [7] Liu Q, Gong M, Cook B, Ewing D, Casper M, Stramel A and Wu J 2017 Transfer-free and printable graphene/ZnO nanoparticle nanohybrid photodetectors with high performance *J. Mater. Chem. C* **5** 6427–32
- [8] Shao D, Yu M, Sun H, Hu T, lian J and Sawyer S 2013 High responsivity, fast ultraviolet photodetector fabricated from ZnO nanoparticle–graphene core–shell structures *Nanoscale* **5** 3664–7
- [9] Safa S, Sarraf-Mamoory R and Azimirad R 2015 Ultra-violet photodetection enhancement based on ZnO–graphene composites fabricated by sonochemical method *J. Sol-Gel Sci. Technol.* **74** 499–506
- [10] Chen C, Zhou P, Wang N, Ma Y and San H 2018 UV-assisted photochemical synthesis of reduced graphene oxide/ZnO nanowires composite for photoresponse enhancement in UV photodetectors *Nanomaterials* **8** 26
- [11] Chang H, Sun Z, Ho K Y-F, Tao X, Yan F, Kwok W-M and Zheng Z 2011 A highly sensitive ultraviolet sensor based on a facile *in situ* solution-grown ZnO nanorod/graphene heterostructure *Nanoscale* **3** 258–64
- [12] Guo D-Y, Shan C-X, Qu S-N and Shen D-Z 2014 Highly sensitive ultraviolet photodetectors fabricated from ZnO quantum dots/carbon nanodots hybrid films *Sci. Rep.* **4** 7469
- [13] Lee S-W *et al* 2016 Low dark current and improved detectivity of hybrid ultraviolet photodetector based on carbon-quantum-dots/zinc-oxide-nanorod composites *Org. Electron.* **39** 250–7
- [14] Woltornist S J, Oyer A J, Carrillo J-M Y, Dobrynin A V and Adamson D H 2013 Conductive thin films of pristine graphene by solvent interface trapping *ACS Nano* **7** 7062–6
- [15] Padmanabhan M, Meyen R, Houghton K and St John M 2018 Solvent interface trapping as an effective technique to fabricate graphite-nanomaterial composite thin films *MRS Advances* **3** 19–23
- [16] Son D I, Yang H Y, Kim T W and Park W I 2013 Photoresponse mechanisms of ultraviolet photodetectors based on colloidal ZnO quantum dot-graphene nanocomposites *Appl. Phys. Lett.* **102** 021105
- [17] Guo W, Xu S, Wu Z, Wang N, Loy M M T and Du S 2013 Oxygen-assisted charge transfer between ZnO quantum dots and graphene *Small* **9** 3031–6
- [18] Liu Y, Gorla C R, Liang S, Emanetoglu N, Lu Y, Shen H and Wraback M 2000 Ultraviolet detectors based on epitaxial ZnO films grown by MOCVD *J. Electron. Mater.* **29** 69–74
- [19] Liang S, Sheng H, Liu Y, Hua Z, Lu Y and Shen H 2001 ZnO Schottky ultraviolet photodetectors *J. Cryst. Growth* **225** 110–3
- [20] Fu X-W, Liao Z-M, Zhou Y-B, Wu H-C, Bie Y-Q, Xu J and Yu D-P 2012 Graphene/ZnO nanowire/graphene vertical structure based fast-response ultraviolet photodetector *Appl. Phys. Lett.* **100** 223114
- [21] Duan L, He F, Tian Y, Sun B, Fan J, Yu X, Ni L, Zhang Y, Chen Y and Zhang W 2017 Fabrication of self-powered fast-response ultraviolet photodetectors based on graphene/ZnO:Al nanorod-array-film structure with stable Schottky barrier *ACS Appl. Mater. Interfaces* **9** 8161–8

- [22] Boruah B D, Ferry D B, Mukherjee A and Misra A 2015 Few-layer graphene/ZnO nanowires based high performance UV photodetector *Nanotechnology* **26** 235703
- [23] Liu Q, Gong M, Cook B, Ewing D, Casper M, Stramel A and Wu J 2017 Fused nanojunctions of electron-depleted ZnO nanoparticles for extraordinary performance in ultraviolet detection *Adv. Mater. Interfaces* **4** 1601064